A EUROPEAN JOURNAL OF CHEMICAL BIOLOGY

CHEMBIOCHEM

SYNTHETIC BIOLOGY & BIO-NANOTECHNOLOGY

Accepted Article

Title: The oxidation of hydrophobic aromatic substrates using a variant of the P450 monooxygenase CYP101B1

Authors: Md Raihan Sarkar, Joel H.Z. Lee, and Stephen Graham Bell

To be cited as: *ChemBioChem* 10.1002/cbic.201700316

Link to VoR: http://dx.doi.org/10.1002/cbic.201700316

A Journal of

ChemPubSoc Europe

WILEY-VCH

www.chembiochem.org

10.1002/cbic.201700316

WILEY-VCH

FULL PAPER

The oxidation of hydrophobic aromatic substrates using a variant of the P450 monooxygenase CYP101B1

Md Raihan Sarkar,[a] Joel H.Z. Lee[a] and Dr Stephen G. Bell[a]

Abstract: The cytochrome P450 monooxygenase CYP101B1, from a *Novosphingobium* bacterium is able to bind and oxidise aromatic substrates but at a lower activity and efficiency compared to norisoprenoids and monoterpenoid esters. Histidine 85 of CYP101B1 aligns with tyrosine 96 of CYP101A1, which in this enzyme forms the only hydrophilic interaction with its substrate, camphor. The histidine residue of CYP101B1 was modified to a phenylalanine with the aim of improving the activity of the enzyme for hydrophobic substrates. The H85F mutant lowered the binding affinity and activity of the enzyme for β-ionone and altered the oxidation selectivity. This variant also showed enhanced affinity and activity towards alkylbenzenes, styrenes and methylnaphthalenes. For example the product formation rate of acenaphthene oxidation was improved 6-fold to 245 nmol.nmol-CYP^{-1}.min^{-1}. Certain disubstituted naphthalenes and substrates such as phenylcyclohexane, and biphenyls, were oxidised with lower activity by the H85F variant. Variants at H85 (A and G) designed to introduce additional space in the active site to accommodate these larger substrates did not engender improvements in the oxidation activity. As the H85F mutant of CYP101B1 improved the oxidation of hydrophobic substrates this residue is likely to be in the substrate binding pocket or the access channel of the enzyme. The side chain of the histidine may interact with the carbonyl groups of the favoured norisoprenoid substrates of CYP101B1.

Introduction

Cytochrome P450 enzymes (CYP), are a large superfamily of heme-dependent monooxygenases which are able to oxidise the inert C-H bonds of organic molecules. This often occurs with high regio- and stereoselectivity. As a result, they have potential roles as catalysts for the synthesis of fine chemicals under mild reaction conditions.[1] CYP enzymes are found across all Kingdoms of life including bacteria, fungi, plants and mammals. The enzymes from bacteria are among the most promising for the selective oxidation of non-functionalised hydrocarbons at high activities.[1f, h, 2] Most CYP enzymes require two electrons, which are usually derived from NAD(P)H. These are delivered to the CYP enzymes one at a time, by electron transfer proteins.[3] For larger scale applications of CYP enzymes the identification and isolation of suitable electron transfer proteins is critical. When efficient electron transfer is combined with an optimal substrate bacterial CYP enzymes have been shown to catalyse their reactions with high activity and efficiency.[2c, 4] For example the self-sufficient CYP102A1 enzyme from *Bacillus megaterium* ($P450_{Bm3}$) catalyses the oxidation of long chain unsaturated fatty acids with exceptionally high rates.[1a, 2c, 4a, 5] The more prevalent Class I CYP enzymes have electron transfer systems which consist of a flavin-dependent ferredoxin reductase and a ferredoxin. This includes CYP101A1 ($P450_{cam}$) from a *Pseudomonas* sp. which can oxidise its substrate, in this case camphor to 5-*exo*-hydroxycamphor, with a product formation activity in excess of 1000 min^{-1}.[6]

Alkyl substituted benzenes and naphthalenes are toxic compounds which also have carcinogenic and mutagenic activities.[7] Acenaphthene and substituted benzene derivatives are utilised for the synthesis of compounds such as plasticizers, resins, polymers, pigments and drug molecules.[8] The selective introduction of a hydroxyl group into the C-H bonds of these substrates by a CYP enzyme, could facilitate these syntheses. In addition, oxidation of these compounds has potential applications in environmental bioremediation.[4f, 6a, 9] Different CYP enzymes have been reported to oxidise naphthalene and benzene derivatives, such as CYP110E1, from *Nostoc* sp. strain PCC7120 and the fungal enzyme CYP63A2 from *Phanerochaete chrysosporium*. The P450 peroxygenase from *Agrocybe aegerita* can also turnover these substrates.[10] While these enzymes were capable of oxidising these substrates the majority of the reactions were non-selective forming multiple products in low yield.[10-11] Mutant forms of CYP101A1 and CYP102A1 (P450Bm3) have been reported to oxidise aliphatic and aromatic molecules such as naphthalene and alkylbenzenes.[6a, c, 9, 11a, 12]

The bacterium *Novosphingobium aromaticivorans* DSM12444 is able to degrade a wide variety of aromatic hydrocarbons. This bacterium contains many monooxygenase encoding genes and dioxygenase enzymes which could have potential applications as biocatalysts.[13] Several of the CYP monooxygenase enzymes, such as CYP101B1, CYP101C1, CYP101D1 and CYP101D2, are related to CYP101A1. CYP101D1 and CYP101D2 oxidise camphor, yielding the same product as CYP101A1. CYP101C1 and CYP101B1 can bind and selectively hydroxylate norisoprenoids. CYP101B1 was able to oxidise camphor but unlike with norisoprenoids the reaction was unselective generating five products. A class I electron transfer system, consisting of a flavin-dependent ferredoxin reductase, ArR, and a [2Fe-2S] ferredoxin, Arx, has been identified from this bacterium which can support the activity of CYP101B1, as well as those of CYP101C1, CYP101D1 and CYP101D2.[2a, 14] With all

[a] Md. Raihan Sarkar, J.H.Z. Lee & Dr. S.G. Bell
Department of Chemistry
University of Adelaide
Adelaide. SA, 5005, Australia
E-mail: stephen.bell@adelaide.edu.au

Supporting information for this article is given via a link at the end of the document.

four CYP enzymes product formation rates in excess of 1000 nmol.nmol P450^{-1}.min^{-1} have been reported. In addition, a whole-cell system has been constructed containing CYP101B1, ArR and Arx. This is capable of product formation on the gram-per-litre scale in shake flasks.[14a]

Further studies showed that CYP101B1 was a flexible biocatalyst with a broad substrate range and can oxidise monoterpenoid and adamantyl esters as well as hydrophobic aromatic compounds such as indole, phenylcyclohexane, *p*-cymene alkylnaphthalenes and methylbiphenyls.[4d, f, 14a, 15] Therefore the CYP101 family enzymes, and in particular CYP101B1, are potential candidates for biocatalytic oxidation of aromatic hydrocarbons. However, the hydrophobic substrates induce a smaller heme spin state shift, bind with lower affinity and are oxidised at slower product formation rates compared to norisoprenoids and the esters. The aim of this study was to improve the activity of the CYP101B1 enzyme for hydrophobic substrates.

Protein engineering of CYP enzymes can be used to enable the oxidation of substrates not normally accepted by the wild-type enzymes.[1e, g, 4a, 16] Crystal structures of CYP101C1, CYP101D1 and CYP101D2 but not CYP101B1 have been solved.[15b, c, 17] The crystal structures of CYP101A1 and CYP101D2 have been used to engineer the enzymes by rational mutagenesis.[1g, 6b, 15b] Notably, CYP101A1 has been used as a model system to demonstrate how changes to the active site of a CYP enzyme can enable the oxidation of hydrophobic substrates of different sizes.[4e, 6c, 12a, 18] By aligning the amino acid sequences of these CYP101 family enzymes we have shown that the tyrosine 96 residue of CYP101A1, which forms a hydrogen bond to the camphor carbonyl group, is conserved in CYP101D1 and CYP101D2 but not CYP101C1 and CYP101B1.[14, 15c, 17a] Here we report that alteration of the histidine residue of CYP101B1, which aligns sequentially with Y96 of CYP101A1, to a phenylalanine increases the efficiency of selective oxidation of a range of hydrophobic alkyl-benzenes and naphthalenes.

Results

The oxidation of alkylbenzenes by CYP101B1 and the H85F variant

The tyrosine 96 residue (Y96) of CYP101A1, which is also conserved in CYP101D1 and CYP101D2, forms a hydrogen bond to the camphor carbonyl group. This is the only hydrophilic interaction between the active site residues of both CYP101A1 and CYP101D1 and the camphor substrate (Fig. 1).[6d] Mutation of this tyrosine residue to remove the hydroxy group enhanced the affinity of CYP101A1 and CYP101D2 for more hydrophobic substrates.[1g, 15b, 18a] The tyrosine residue aligns with a methionine residue in CYP101C1 (M82) and a histidine in CYP101B1 (H85).[15c] We hypothesised that H85 of CYP101B1 may play a similar role interacting with norisoprenoid and ester substrates potentially through the carbonyl group.[4d, 15a, c] Replacing H85 with a more hydrophobic residue, such as phenylalanine, could therefore, improve the affinity of CYP101B1 towards hydrophobic aromatic compounds. The H85F variant of CYP101B1 was made and tested alongside the WT enzyme with a range of hydrophobic aromatic compounds and the norisoprenoid β-ionone (Fig. 2).

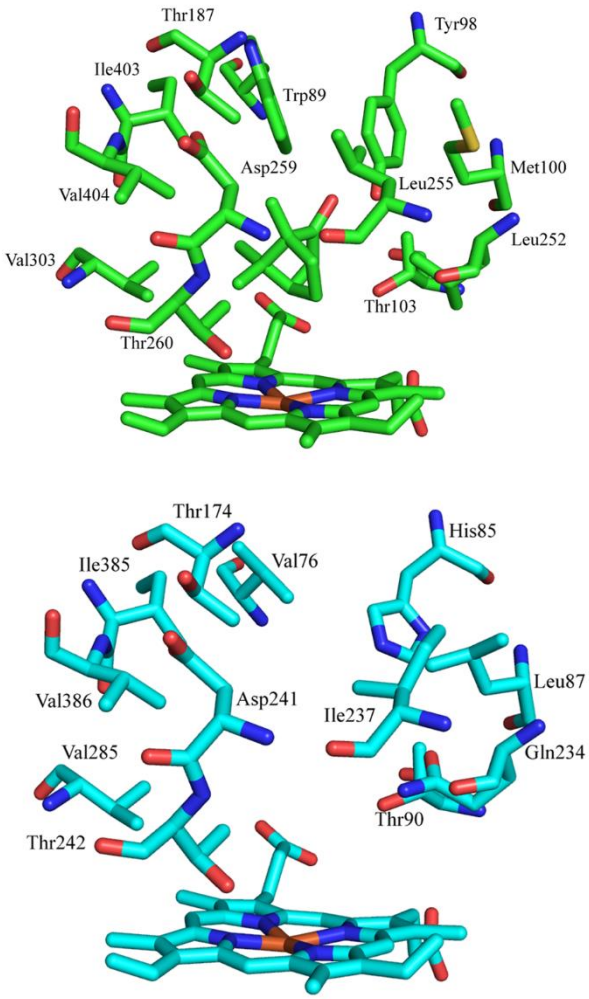

Figure 1 (top) the crystal structure of camphor bound CYP101D1 (PDB 3LXI) highlighting the hydrogen bond interaction between the camphor carbonyl and the conserved tyrosine residue (Y98). This is the equivalent residue to Y96 in CYP101A1. CYP101D1 was the closest homologue of CYP101B1 in the PDB. (bottom). The modelled structure of CYP101B1 created using Swiss Model highlighting the potential location of histidine 85 (H85).

The spin state shift and binding affinity of the H85F mutant with *β*-ionone was reduced compared to the WT enzyme. The oxidation activity was almost 10-fold lower (Table 1). In addition the selectivity of oxidation was also altered. While the WT enzyme favoured generation of the 3-hydroxy metabolite the H85F variant catalysed hydroxylation mainly at the more reactive allylic C-H bonds to produce 4-hydroxy-*β*-ionone (Scheme 1, Fig. S3(a)).[2a, 14a, 15c]

WT CYP101B1 can oxidise *p*-cymene and indole and so we tested a range of similarly sized alkylbenzene substrates with the H85F variant (Table 1).[15c] The effect of the size and position of

the alkyl substituent on binding and activity parameters was investigated using isobutylbenzene, *n*-propyl- and isopropylbenzene, 2- and 3-ethyltoluene and indane (Fig. 2). Styrene, 2-methylstyrene and *β*-methylstyrene were tested to examine the effect of the planar and more reactive vinyl substituent (Fig. 2).

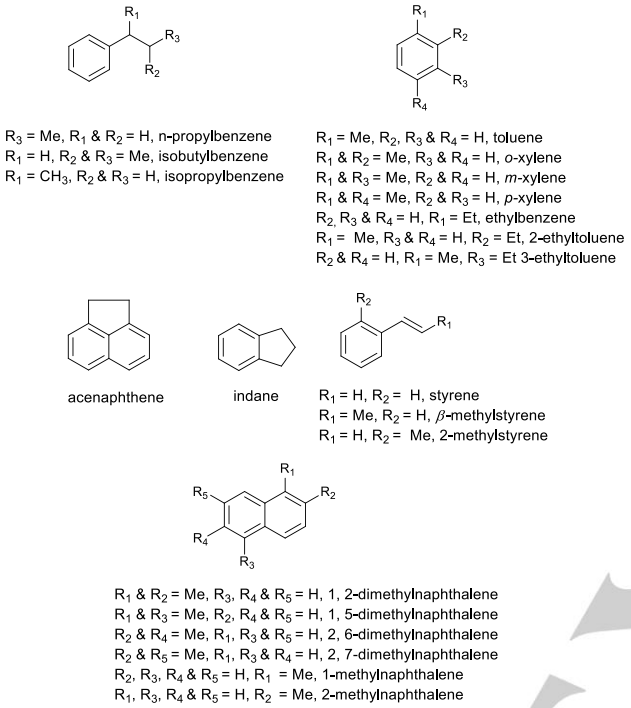

Figure 2 The substrates tested for activity with WT CYP101B1 and H85F CYP101B1

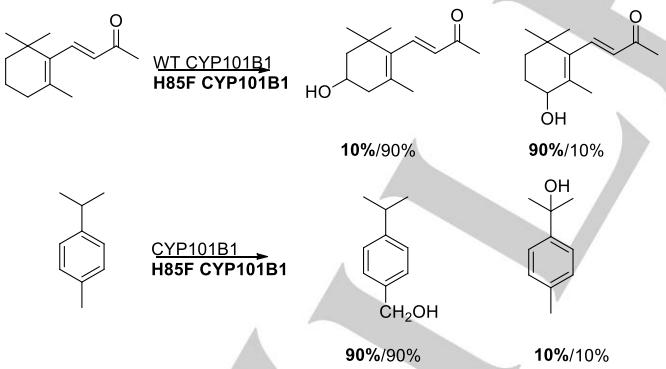

Scheme 1 The products identified from the CYP101B1 and H85F CYP101B1 turnovers of β-ionone and p-cymene. The product distributions are given as percentages (H85F variant in bold).

The spin state shift induced by substrate binding was used as an indicator of whether the H85F variant of CYP101B1 was able to better accommodate these hydrophobic substrates. The shift induced in the WT enzyme was minimal across all the substrates, with the maximum switch of ~20% high spin (HS) being observed for indane and *β*-methylstyrene (Table 1 and Table S1). These are significantly lower than the shifts induced by norisoprenoids and monoterpenoid esters (≥95 % HS).[15a, c] The shift induced by these substrates in the H85F variant was greater in almost all cases (Table 1). The exceptions were toluene and 3-ethyltoluene where a 5% HS shift was observed with both variants. In some instances such as *p*-cymene and styrene the increase in the shift was minimal (10% *vs*. 5% HS) but for several substrates it was more substantial, for example ethylbenzene (30% *vs*. 5% HS) and 2-methylstyrene (20% *vs*. 5%). The largest improvements were observed with indane (65% *vs*. 20% HS). The dissociation constants were determined for a selection of the substrates with showed higher spin-state shifts. In all cases the affinity of the H85F variant was significantly higher (Table 1).

In line with the larger spin state shifts observed with the H85F variant the activity of substrate oxidation improved in the majority of cases. For every alkylbenzene tested the NADH oxidation rate was greater for the mutant form of CYP101B1 (Table 1 and Table S1). In all but one instance the coupling efficiency, which is the amount of product formed compared to the NADH reducing equivalent consumed, also increased resulting in greater productive monooxygenase activity (Table 1).

The activity of toluene and xylene substrates were low with both the WT enzyme and the H85F variant (Table 1 and Table S1). By far the best of these smaller substrates was *o*-xylene which was had a PFR of 70 nmol.nmol-CYP^{-1}.min^{-1} (henceforth abbreviated to min^{-1}) with the mutant. The product formation rates for the WT enzyme with the other alkylbenzenes and styrenes varied from 6 to 65 min^{-1} while for the H85F variant the range was 33 to 262 min^{-1}. The largest improvements in the product formation activity (around 5 to 7-fold) were observed for 2-ethyltoluene, 3-ethyltoluene, ethylbenzene, 2-methylstyrene and indane (Table 1). *β*-Methylstyrene was the exception and its activity with the H85F variant was lower than that obtained with the WT due to a reduction in the coupling efficiency.

GC analysis of the *in vitro* turnover of *p*-cymene by the H85F mutant revealed two products (4-isopropyl benzyl alcohol and *p*-α,α-trimethyl benzyl alcohol) in a similar ratio to the WT enzyme (Scheme 1, Fig. S3(b)).[15c] One product arose from the ethylbenzene turnovers, which coeluted with 1-phenylethanol (m^+/z = 122.05) (Scheme 2, Fig. S3(c), Fig. S4). Chiral GC analysis showed that turnover of ethylbenzene generated a mixture of enantiomers; (*S*)-1-phenylethanol and (*R*)-1-phenylethanol in a distribution of 55 to 45%, (Scheme 2, Fig. S3(c)). The H85F variant also generated 1-phenylethanol as a single product but the enantioselectivity of the reaction changed with the (*S*)-1-phenylethanol being produced in excess over (*R*)-1-phenylethanol (77:23).

The toluene and xylenes were all selectively oxidised to a single major product with hydroxylation occurring at the benzylic C–H bonds in all cases (Scheme 2, Scheme S1 and Fig. S3(d-g)). The major product arising from 2-ethyltoluene oxidation was (2-ethylphenyl)methanol, which was identified by NMR after isolation and purification from a whole-cell biotransformation (82% of the total product for the H85F mutant and 88% for WT, m^+/z = 135.95AMU, Fig. S3(h), S4, S5, Scheme 2). 1-(2-Methylphenyl)ethanol (m^+/z = 136.05), which made up the majority of the remaining metabolites, was identified by coelution with a standard (Fig. S3(h)). Chiral GC analysis showed the

Table 1. Substrate binding, turnover and coupling efficiency data for the turnovers of CYP101B1 (WT and the H85F variant) with alkylbenzenes and *β*-ionone. The turnover activities were measured using an ArR:Arx:CYP101B1 concentration ratio of 1:10:1 (0.5 μM CYP enzyme, 50 mM Tris, pH 7.4) 0.5 or 1 mM substrate and ~320 μM NADH. N is the NADH oxidation rate, PFR the product formation rate and C is the coupling efficiency, which is the percentage of NADH utilised for the formation of products. Rates are reported as mean ± S.D. (n ≥ 3) and given in nmol.nmol-CYP^{-1}.min^{-1}. – not measured or not able to be determined accurately.

substrate	CYP101B1	%HS heme	K_d (μM)	N (min^{-1})	PFR (min^{-1})	C %
β-ionone	WT	≥95%	0.23 ± 0.1	1600 ± 100	1010 ± 60	63
	H85F	**50%**	**5.8 ± 2**	**412 ± 36**	**140 ± 11**	**34**
toluene	WT	5%	-	40 ± 6	1 ± 1	2
	H85F	**5%**	**-**	**69 ± 7**	**3 ± 1**	**4**
o-xylene	WT	≤5%	-	55 ± 14	3 ± 1	4
	H85F	**15%**	**-**	**286 ± 4**	**70 ± 3**	**25**
2-ethyltoluene	WT	10%	-	156 ± 7	55 ± 1	35
	H85F	**30%**	**-**	**496 ± 16**	**262 ± 15**	**53**
3-ethyltoluene	WT	≤5%	-	90 ± 13	15 ± 1	16
	H85F	**5%**	**-**	**228 ± 5**	**100 ± 3**	**44**
ethylbenzene	WT	≤5%	520 ± 70	47 ± 2	6 ± 6	13
	H85F	**30%**	**2.5 ± 1**	**201 ± 22**	**43 ± 4**	**21**
n-propylbenzene	WT	≤5%	410 ± 70	121 ± 6	9 ± 5	4
	H85F	**30%**	**0.6 ± 0.1**	**510 ± 13**	**44 ± 4**	**9**
isopropylbenzene	WT	5%	-	98 ± 12	14 ± 1	12
	H85F	**20%**	**-**	**381 ± 8**	**46 ± 2**	**15**
isobutylbenzene	WT	≤5%	70 ± 20	156 ± 2	65 ± 4	42
	H85F	**20%**	**0.9 ± 0.1**	**254 ± 4**	**108 ± 3**	**43**
styrene	WT	≤5%	-	105 ± 2	14 ± 10	13
	H85F	**10%**	**-**	**153 ± 7**	**55 ± 7**	**36**
2-methylstyrene	WT	5%	450 ± 70	161 ± 9	42 ± 3	26
	H85F	**20%**	**13 ± 4**	**405 ± 16**	**219 ± 17**	**54**
β-methylstyrene	WT	10%	395 ± 25	76 ± 6	54 ± 17	71
	H85F	**35%**	**1.8 ± 3**	**90 ± 1**	**33 ± 3**	**37**
p-cymene	WT[15c]	5%	-	197 ± 27	25 ± 6	13
	H85F	**10%**	**-**	**272 ± 11**	**95 ± 7**	**35**
indane	WT	20%	99 ± 11	118 ± 21	28 ± 3	24
	H85F	**65%**	**9.5 ± 7**	**363 ± 8**	**174 ± 9**	**48**

formation of equal amounts of each enantiomer of 1-(2-methylphenyl)ethanol by WT CYP101B1 but that the H85F mutant had a preference (88:12) for the later eluting species (Scheme 1 and Fig. S3 (h)). No standard was available for the other minor product (less than 5%) and we were not able to generate enough for purification and NMR analysis. The MS fragmentation indicated this product was likely to be 2-ethylbenzaldehyde (m^+/z = 136.10, Fig. S4).

Two products arose from oxidation of 3-ethyltoluene by the H85F mutant but three were observed with WT CYP101B1 (Scheme 2, Fig. S3(i)). Whole-cell oxidation was used to generate the products in larger quantities. After purification the products were identified via NMR or coelution experiments and analysis of the MS (Fig. S4 and Fig. S5). The two products common to both enzymes were 1-(3-methylphenyl)ethanol (m^+/z = 136.05) and (3-ethylphenyl)methanol (m^+/z = 136.05) with the latter being formed in excess in both cases (Scheme 2). The additional minor product found in the WT turnover (14% of total product) was characterised by NMR and MS analysis as 2-ethyl-4-methylphenol (m^+/z = 136.05, Scheme 2, Fig. S4, Fig. S5c).[19]

The longer alkyl side chains of *n*-propylbenzene and isobutylbenzene resulted in changes in the product distribution. *n*-Propylbenzene was oxidised to three products, two of which were identified by coelution with 1-phenyl-1-propanol (m^+/z = 136.0) and the further oxidation product propiophenone (m^+/z = 134.05) (Scheme 3, Fig. S3(j) and Fig. S4). The propiophenone further oxidation product was formed in excess for each variant (Scheme 3). The third metabolite was identified, by coelution with the product from the reduction of phenylacetone and MS analysis, as 1-phenylpropan-2-ol (m^+/z = 136.0, Fig. S4). A single product was generated in both the H85F and WT turnover of isobutylbenzene and isopropylbenzene which coeluted with 2-methyl-1-phenyl-2-propanol and 2-phenyl-2-propanol, respectively (Scheme 3, Fig. S3(k), Fig. S3(l), Fig. S4). The cyclic alkylbenzene indane was turned over to two products which coeluted with a 1-indanol and 1-indanone standards (Scheme 1, Fig. S3(m), Fig. S4).

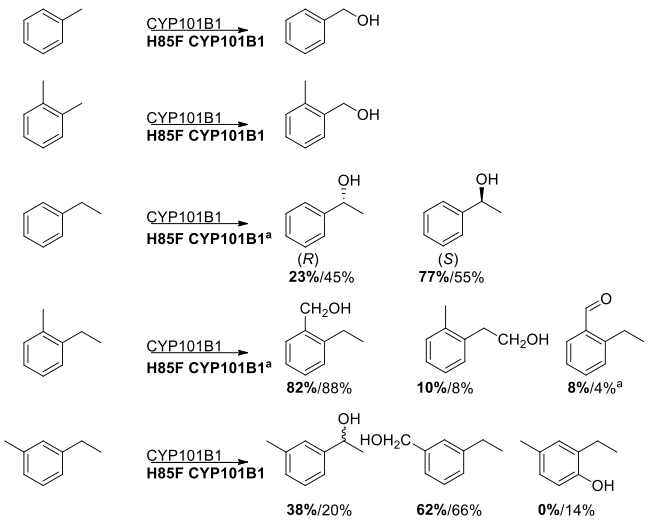

Scheme 2 The products identified from the CYP101B1 and H85F CYP101B1 turnovers of the methyl- and ethyl-benzene like substrates. The product distributions are given as percentages (H85F variant in bold). [a] The WT generated a roughly 50:50 mixture of both enantiomers whereas the H85F variant had 88:12 ratio of one enantiomer (assigned the (*S*) over the other). [a] With ethylbenzene and 2-ethyltoluene very small levels of a potential desaturation product (<1%) could be detected in the turnovers (Fig. S3(c) and S3(h).

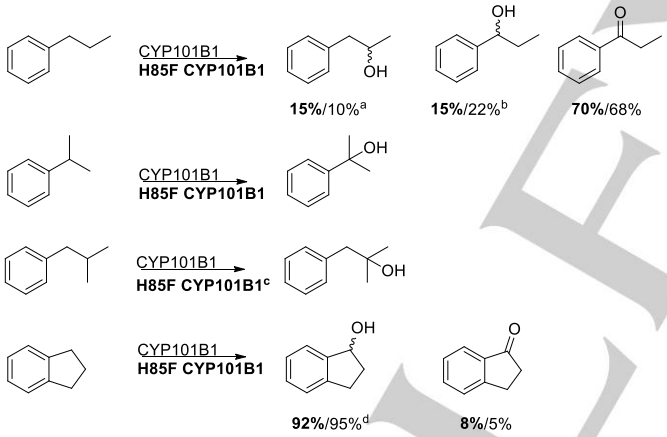

Scheme 3 The products identified from the turnovers of *n*-propyl-, isopropyl, isobutyl-benzene and indane by the WT CYP101B1 and H85F CYP101B1 enzymes. The product distributions are given as percentages (H85F variant in bold).[a] Not separated by chiral GC. [b] The WT generated a 40:60 mixture of each enantiomer whereas the H85F variant had 26:74 ratio the enantiomer in excess was assigned as the (*S*).[c] With isobutylbenzene very small levels of a potential desaturation product (<1%) could be detected in the turnovers. [d] Chiral HPLC revealed that the WT CYP101B1 generated a slight access of one enantiomer whereas the H85F variant had larger excess of the same enantiomer (approx. 70:30, Fig. S3(m)).

Styrene oxidation generated a major product which coeluted phenyloxirane (m^+/z = 120.15). With the H85F mutant a minor product (less than 1%) identified from its MS fragmentation pattern as phenylacetaldehyde (m^+/z = 120.10) was also observed (Scheme 4, Fig. S3(m)). Chiral GC analysis of both sets of turnovers revealed formation of roughly equal mixture of (*S*)-(-)-phenyloxirane and (*R*)-(+)-phenyloxirane (Fig. S3(n)). The enzyme catalysed turnovers of *β*-methylstyrene by WT and H85F produced two major metabolites (Scheme 4 and Fig. S3(n)). The major product in each was confirmed by coelution as 3-phenyl-2-propen-1-ol (Fig. S3). The other product was the epoxide, 2-methyl-3-phenyloxirane (m^+/z = 134.0) and this was identified by analysing the mass spectra and coelution experiments with the reaction of *β*-methylstyrene with *m*-chloroperbenzoic acid (*m*-CPBA; Scheme 1, Fig. S3, Fig. S4).[20] Chiral GC analysis revealed a mixture of two stereoisomers (*R*,*R*)- and (*S*,*S*)-2-methyl-3-phenyloxirane).[21] 2-Methylstyrene generated a single major metabolite (>95%) which was identified as the two enantiomers of the epoxide 2-(2-methylphenyl)oxirane (m^+/z = 134.05; Scheme 1, Fig. S3 and Fig. S4). The minor product was assigned as 2-methylphenylacetaldehyde (m^+/z = 134.05) based on its MS fragmentation pattern (Scheme 1 and Fig. S4).

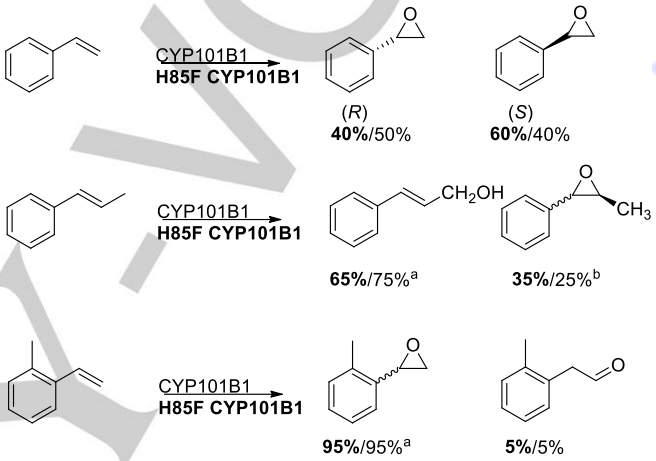

Scheme 4 The products identified from the turnovers of styrene and β-methylstyrene by the WT CYP101B1 and H85F CYP101B1 enzymes. . The product distributions are given as percentages (H85F variant in bold). [a] WT and the H85F variant generated a 60:40 and 55:45 mixture of each enantiomer, respectively. [b] Both the WT and H85F variants generated a 50:50 mixture of each enantiomer.

The oxidation of naphthalene derivatives and related molecules

WT CYP101B1 selectively oxidised 2,7-dimethylnaphthalene, 1- and 2–methylnaphthalene and substituted biphenyls.[15d] The substrate binding and enzymatic activity of WT and the H85F mutant of CYP101B1 was therefore tested with a range of substituent naphthalenes, biphenyls and related molecules such as phenylcyclohexane (Fig. 1). The addition of 1- and 2-methylnaphthalene, acenaphthene and 1,5- and 2,6-dimethylnaphthalene induced larger spin state shifts in the variant than the WT enzyme (Table 2.Fig. S1 and S2). However the opposite trend was observed with 2,7-dimethylnaphthalene and 1,2-dimethylnaphthalene (Table S1). Where measured, the binding affinity of these substrates with the H85F variant was higher, no matter whether the spin state shift was improved or not (Table 2, Table S1 and Fig. S2). Mixed results were also observed with other substrates tested; for example, the spin state shift induced by phenylcylcohexane was lower with the H85F mutant than the WT enzyme while moderate increases were observed with 2-, 3- and 4-methylbiphenyl (Table S1).

Table 2 Substrate binding, turnover and coupling efficiency data for the turnovers of CYP101B1 (WT and the H85F variant) with alkyl substituted naphthalenes. The turnover activities were measured using an ArR:Arx:CYP101B1 concentration ratio of 1:10:1 (0.5 μM CYP enzyme, 50 mM Tris, pH 7.4)) 0.5 mM substrate and ~320 μM NADH. N is the NADH oxidation rate, PFR the product formation rate and C is the coupling efficiency, which is the percentage of NADH utilised for the formation of products. Rates are reported as mean ± S.D. (n ≥ 3) and given in nmol.nmol-CYP^{-1}.min^{-1}. – not measured.

substrate	CYP101B1	%HS heme	K_d (μM)	N (min^{-1})	PFR (min^{-1})	C %
1,2-dimethylnaphthalene	WT	55%	20 ± 4	136 ± 13	25 ± 2	19
	H85F	**40%**	**2.4 ± 0.1**	**242 ± 8**	**57 ± 2**	**24**
1,5-dimethylnaphthalene	WT	55%	28 ± 3	135 ± 5	17 ± 1	13
	H85F	**80%**	**2.6 ± 0.2**	**355 ± 30**	**84 ± 12**	**24**
2,6-dimethylnaphthalene	WT	10%	-	113 ± 5	23 ± 1	21
	H85F	**20%**	**-**	**76 ± 13**	**3 ±1**	**4**
acenaphthene	WT	30%	20 ± 4	165 ± 24	42 ± 7	25
	H85F	**60%**	**5.9 ± 0.6**	**513 ± 16**	**245 ± 12**	**48**
1-methylnaphathelene	WT[15d]	50%	63 ± 9	240 ± 17	38 ± 10	16
	H85F	**60%**	**3.3 ± 0.4**	**453 ± 25**	**161 ± 13**	**36**
2-methylnaphathelene	WT[15d]	30%	135 ± 10	212 ± 24	57 ± 18	26
	H85F	**50%**	**16.1 ± 6**	**158 ± 13**	**32 ± 3**	**20**

In general the activity of oxidation for the alkylnaphthalenes varied in line with the trend in the spin state induced by the substrate. For example 1,2-dimethylnaphthalene, 1,5-dimethylnaphthalene, acenaphthene and 1-methylnaphthalene all showed a higher product formation rate with H85F mutant compared to the WT (Table 2). These arose through an increase in the rate of catalytic turnover, as measured by NADH oxidation, and the coupling efficiency. For 1,2-dimethylnaphthalene the biocatalytic properties were moderately enhanced for the H85F variant over the WT, despite the lower spin state shift. 2-Methylnaphthalene and 2,6-dimethylnaphthalene both had lower NADH oxidation rates, coupling efficiencies and product formation rates with the H85F mutant. The product formation activity of phenylcyclohexane and all the biphenyls tested with the H85F variant were inferior compared to the WT enzyme (Table S1).

The oxidation of all the substituted naphthalenes by WT and the H85F variant of CYP101B1 were regioselective. The oxidation of 1- and 2-methylnaphthalene generated 1- and 2-naphthylmethanol, respectively, which were identified by coelution with standards (Fig. S3(q) and Fig. S3(r)). The product of 1,2-dimethylnaphthalene oxidation was characterised after a whole-cell biotransformation to generate the metabolite on a larger scale (Fig. S3(s)). The product was confirmed as (1-methyl-2-naphthyl)methanol (m^+/z = 172.05) by comparing the NMR to that published previously (Fig. S5).[22] Whole-cell oxidation was also used to generate the sole products formed after oxidation of 1,5- and 2,6-dimethylnaphthalene (Fig. S3(t) and Fig. S3(u)). These were isolated and identified by NMR as (5-methyl-1-naphthyl)methanol (m^+/z = 172.0) and (6-methyl-2-naphthyl)methanol (m^+/z = 172.05), respectively (Scheme 5, Fig. S3, Fig. S4, Fig. S5). The product of acenaphthene was also isolated and identified by NMR as 1-acenaphthol (m/z = 172.05, Scheme 5, Fig. S3(v), Fig. S4 and Fig. S4). The enantioselectivity of the reaction was investigated by HPLC. The WT enzyme and the H85F variant generated a 70:30 and 60:40 ratio of each enantiomer, respectively (Fig. S3(v)).

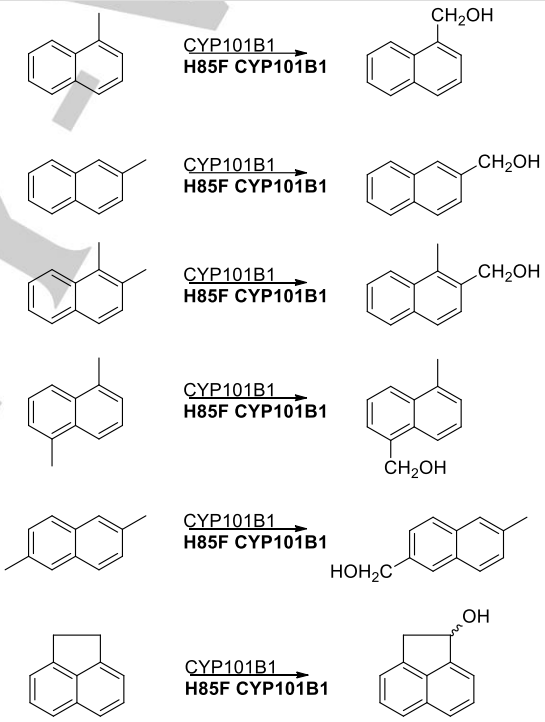

Scheme 5 The products identified from the CYP101B1 and H85F CYP101B1 turnovers of the alkylnaphthalenes.

The turnovers with the biphenyl compounds, phenylcyclohexane and 2,7-dimethylnaphthalene with the mutant all generated lower levels of oxidised metabolites compared to the WT CYP101B1 enzyme. 4-Methylbiphenyl generated 4-biphenylmethanol as the major product with the H85F variant in contrast to the WT which produced a greater proportion of 4′-(4-methylphenyl)phenol as the major product (Fig. S3(w), Scheme S2).[15d] There were no changes in the product distribution with the H85F variant of CYP101B1 with 2,7-dimethylnaphthalene, phenylcyclohexane and the other biphenyls compared to the WT enzyme (Fig. S3(x)).[15d]

Given the reduced activity of the H85F variant for the larger phenylcyclohexane, naphthalene and biphenyl molecules we made the H85A and H85G mutants of CYP101B1. These would by analogy with the Y96A variant of CYP101A1 be expected to increase the volume of the active site enabling larger substrates to be efficiently oxidised.[6c, 12a, 18a] Both variants were shown to be functional P450s (Fig. S6) and were tested with a range of substrates including *β*-ionone and phenylcyclohexane (supporting information). Both variants had reduced activity for *β*-ionone oxidation compared to the WT enzyme and the product selectivity was similar to that of the H85F variant (Table S2 and Fig. S7). With the hydrophobic phenylcyclohexane the spin-state shift and or the binding affinity were lower than the WT forms of CYP101B1 (Table S2). In addition less product was generated by these variants at a lower activity. These trends in binding affinity and product formation were consistent across the other hydrophobic substrates tested no matter their size (data not shown).

Discussion

The results indicated that alkylbenzenes and certain methylnaphthalenes bound more readily in the active site of the H85F mutant of CYP101B1. As a result many of these substrates were oxidised to products with higher activity compared to the WT enzyme. For most hydrophobic compounds tested the NADH oxidation rate increased for the mutated form, in line with the greater spin state shift, which suggests that substrate binding is playing a role in gating the commencement of the catalytic cycle.[23] The product formation rates of some substrates was relatively high despite inducing lower spin state shifts. This suggest that the gating mechanism in CYP101B1 may be less stringent than is observed in other systems such as CYP101A1.[24] This is in agreement with results obtained for other CYP101 family enzymes.[14b, 17a] When incorporated into whole-cell biotransformation system, with the physiological electron transfer partners, ArR/Arx and the CYP101B1 H85F variant was capable of synthesising the oxidised metabolites of alkylbenzenes and naphthalenes in good yields for characterisation (18-33 mg of purified naphthalene metabolites were generated from 200 ml of culture after a 16 h reaction performed as described in the experimental section).

In general the selectivity of substrate oxidation by the H85F variant was similar to that of the WT enzyme. In certain instances changes in the regio- and stereo-selectivity of product formation were observed with the mutant enzyme. The oxidation of *β*-ionone by the H85 variants was lower than the WT enzyme and the selectivity was altered. The H85F variant was 90% selective for hydroxylation at the allylic C-H bond, generating 4-hydroxy-β-ionone in contrast to the WT enzyme was produced 3-hydroxy-β-ionone in excess (90%). This suggests that the histidine 85 residue of CYP101B1 must be in the active site or the access channel of CYP101B1 and that it interacts with the substrate to control its binding orientation. Larger molecules such as phenylcyclohexane and biphenyls were poorer substrates for the H85F variant which suggests that this mutation may result in less available space for substrate binding.

The oxidation of ethylbenzene, acenaphthene, indane and alkylnaphthalenes were selective for hydroxylation of a benzylic C–H bond. Addition of substituents on the benzene ring altered the selectivity with the observation of competition between two alkyl substituents. It is of note that the major product for 2- and 3-ethyltoluene arose from oxidation at the less reactive methyl substituent which was consistent with the reactivity observed with *p*-cymene, suggesting a preference for oxidation at benzylic methyl groups over longer chain alkyl groups. The presence of the alkene bond of styrenes resulted in epoxidation. However cinnamyl alcohol was the major product arising from oxidation of *β*-methylstyrene suggesting that the allylic methyl group of this substrate must be located significantly closer to the heme iron that the more reactive alkene. The increased flexibility of *n*-propylbenzene resulted in preferential hydroxylation at the benzylic position though the major product was the ketone further oxidation product. Isobutylbenzene hydroxylation was shifted to the tertiary *β*-carbon and the branching in the alkyl chain must alter the binding orientation of substrate in the vicinity of the heme iron. The oxidation of *o*-xylene and related substrates occurred without any observation of products arising from a 1,2-shift and minimal desaturation of alkyl chains (< 1%) was observed; reactions which occur with CYP102A1.[12b, c, 19] The ability of CYP101B1 to favour hydroxylation at less reactive positions in certain substrates may make it a useful for future synthetic applications.

Alteration of H85 to amino acid residues with smaller side chains (alanine and glycine) did not lead to an enhancement in the binding or the activity of the enzyme for the larger substrates tested. This was somewhat surprising given the ability of the Y96A mutant of CYP101A1 to accept larger molecules such as diphenylmethane. However we note that the Y96A variant of CYP101D2, also from *N. aromaticivorans*, does not improve the activity for larger substrates either.[15b] Mutations at other residues in the active site of CYP101B1 could be used to generate variants that could bind and oxidise larger hydrophobic substrates. For example glutamine 234 and isoleucine 237 align with leucine 244 and valine 247 of CYP101A1 which have been modified to increase the activity of this enzyme for unnatural substrates. It is worth noting that studies on the equivalent residues of CYP101D2 designed to increase the affinity for camphor did not enhance substrate binding in this enzyme.[15b] The contrasting behaviour of the CYP101 family members from different bacteria suggests that the mutations may have a distinctive effect on the conformation of the enzymes. This could arise from divergent interactions of the residues constituting and surrounding the active site. This provides further evidence that the evolution of P450 substrate specificity and function depends on other factors than simply the identity of the residues which constitute the first sphere of the binding pocket and their interactions with the substrate.

Conclusions

In summary, replacement of histidine 85 of CYP101B1 with hydrophobic phenylalanine improved the binding of and product formation activity with hydrophobic substrates including alkylbenzenes and naphthalenes. Histidine must be located in the active site or access channel of the CYP101B1 enzyme. There was a selectivity preference for oxidation at benzylic methyl groups over other alkyl substituents when both were present. The enzyme could also oxidise branched alkyl side chains and β-substituted styrenes at less reactive positions. These mutagenesis experiments could be expanded to enable the development of biocatalytic routes to synthesise fine chemicals arising from the oxidation of aromatic substrates.

Experimental Section

General reagents and organics were from Sigma-Aldrich, Acros, TCI or VWR. Buffer components (Tris-HCl) NADH, and isopropyl-β-D-thiogalactopyranoside (IPTG) were from Anachem (Astral Scientific, Australia) or Biovectra, (Scimar, Australia). General DNA manipulations and microbiological experiments and the expression, purification and quantitation of CYP101B1 and the electron transfer proteins ArR and Arx were performed using standard methods as described previously.[2a, 6b, 14a, 25] A Varian Cary 5000 or Agilent Cary 60 spectrophotometer was used for UV/Vis spectroscopy. Gas chromatography (GC-MS) analyses were carried out on a Shimadzu GC-17A instrument coupled to a QP5050A MS detector using a DB-5 MS fused silica column (30 m x 0.25 mm, 0.25 µm) and helium as the carrier gas (flow rate 1.2 ml min^{-1}). The injector and interface temperatures were 250 °C and 280 °C, respectively. The initial oven temperature of 80°C or 120 °C was held for 3 min before being raised at 10 min^{-1} to 220 °C min^{-1} where it was maintained for 7 min. For chiral GC analysis (β-DEX column; 30 m x 0.25 mm, 0.25 µm) was performed on a Shimadzu Tracera system equipped with a BID detector. The injector and BID temperatures were both 230 °C with the initial oven temperature of 80 °C being held for 3 min before being raised at 5 min^{-1} to 200 °C min^{-1} where it was maintained for 3 min.

Analytical High Performance Liquid Chromatography (HPLC) was performed on an Agilent 1260 Infinity Pump equipped with an autoinjector connected using an Agilent Eclipse Plus C18 column (250 mm x 4.6 mm, 5 µm). The products were separated using a gradient between 20 – 95%, acetonitrile in water (0.1% trifluoroacetic acid (TFA) at a flow rate of 1 mL min^{-1} over 30 minutes. For chiral analysis a Lux 3u cellulose-1 column (100 x 4.6 mm) was used with a gradient between 10 – 100%, acetonitrile in water (0.1% trifluoroacetic acid (TFA) at a flow rate of 0.4 mL min^{-1} over 50 minutes. Additional normal phase chiral chromatography was carried out on a Shimadzu LC20-AR system equipped with a UV-Vis dectector and a ChiralPak IG column (5 µm, 150 x 4.6 mm). Hexane was used as the mobile phase with a gradient of isopropanol (0 – 12%) at a flow rate of 0.4 mL min^{-1} over 38 min. NMR spectra were acquired on an Agilent DD2 spectrometer operating at 500 MHz for ^{1}H and 126 MHz for ^{13}C.

Protein engineering

Sequence alignment showing that histidine 85 of CYP101B1 aligns with tyrosine 96 of CYP101A1 has been carried out and reported previously.[15c] The active site of CYP101B1 was derived using Swiss-Model using the CYP101D1 structure as a model (Fig. 1).[26] The gene encoding CYP101B1 H85F was codon optimised and purchased as a gblock from Integrated DNA Technology (IDT, supporting information). NdeI and HindIII sites were added at the 5′ and 3′ termini, respectively and these were used to clone the gene into the pET26 vector (Novagen). A SalI restriction site (silent mutation) was incorporated into the gene at the base pairs equivalent to the amino acid residues 125-126 to enable the cloning of other H85 variants using shorter gblocks fragments (Supporting information).

Substrate binding and activity measurements

To determine the magnitude of any spin state shift, the enzyme was diluted to ~2 µM using 50 mM Tris, pH 7.4. Aliquots of substrate (0.5 to 1 µL) were added from 100 mm stock solution in ethanol or DMSO and the absorbance was monitored from 700 nm to 250 nm. The proportion of high spin ferric iron was determined, to approximately ±5%, by comparison with a set of spectra generated from the sum of the appropriate percentages of the spectra of the substrate-free form (>95% low spin, Soret maximum at 418 nm) and camphor-bound form of $P450_{cam}$ (>95% high spin, Soret maximum at 392 nm).[27]

The dissociation constants were determined by measuring the difference spectrum upon addition of increasing amounts of substrate. Aliquots of 0.5 ~ 2 µL were added using a Hamilton syringe from a 1, 10 or 50 mM stock solution in DMSO or ethanol, into 2.1 µM of enzyme in a total volume of 2.5 mL in 50 mM Tris, pH 7.4. The solution was mixed and the peak-to-trough difference in absorbance recorded between 700 nm and 250 nm until this did not shift further. The dissociation constant, K_d, was calculated by fitting the peak-to-trough difference against substrate concentration to a hyperbolic function (Eqn. 1):

$$\Delta A = \frac{\Delta A_{max} \times [S]}{K_d + [S]}$$

where ΔA is the peak-to-trough absorbance difference, ΔA_{max} is the maximum absorbance difference and [S] is the substrate concentration.

For substrates which exhibited tight binding to the H85F variant, with $K_d <$ 5[E], the data were fitted to the tight binding quadratic equation (Eqn. 2) [28]:

$$\frac{\Delta A}{\Delta A_{max}} = \frac{([E]+[S]+K_d) - \sqrt{\{([E]+[S]+K_d)^2 - 4[E][S]\}}}{2[E]}$$

where ΔA is the peak-to-trough absorbance difference, ΔA_{max} is the maximum absorbance difference, [S] is the substrate concentration and [E] is the enzyme concentration.

In vitro NADH turnovers were performed in a total volume of 1.2 mL containing the CYP enzyme (0.5 µM), Arx (5 µM), ArR (0.5 µM), bovine liver catalase (100 µg mL^{-1}) and oxygenated 50 mM Tris (pH 7.4). The mixture was allowed to reach 30 °C before the addition of substrate to a final concentration of 0.5 mM. NADH was added, to initiate the turnover, at a concentration of ~320 µM (which corresponds to an A_{340} of ~2) and the absorbance at this wavelength was recorded. The rate of NADH oxidation was calculated using ε_{340} = 6.22 mM^{-1} cm^{-1}. A 1 ml aliquot of the turnover was removed and 10 µL of an internal standard (*p*-cresol, from a 20 mM stock solution was added). The products were extracted with 400 µL ethyl acetate. The organic extract was separated, collected and analysed via GC-MS (see supporting information for details and retention times). When an authentic standard was available products were identified by coelution experiments and matching of the mass spectrum. Otherwise the product was isolated after whole-cell oxidation and characterised via NMR. For minor products the MS fragmentation pattern was used for identification purposes. The amount of product was quantitated by performing calibrations with an authentic standard or an isomer. Where multiple products were generated the detector response was assumed to

be equal for isomeric metabolites. The coupling efficiency was calculated as the percentage of NADH used to generate product.

Product isolation and characterisation

Whole-cell turnovers were used to synthesise products on a larger scale for characterisation when standards were not available. The plasmid pETDuetArx/ArR was combined in *E. coli* with pRSFDuetArx/CYP101B1 or pRSFDuetArx/H85FCYP101B1 and used in a whole-cell turnover to generate metabolites.[6b, 14a] The growths and protein induction were conducted on a 100 ml scale using 2xYT media as described previously.[15a, c, d] The cells were harvested by centrifugation (8 g of cell wet weight per litre, P450 concentration ~650 nM) and resuspended in 200 ml *E. coli* minimal media (EMM). The resuspended cells and substrate (0.5 - 2 mM) were added to a 2 L baffled flask and shaken at 150 rpm at 30 °C for 16 hours. Two further aliquots of substrate (same amount as the initial addition were added after 3 and 6 hours). The supernatant was extracted in ethyl acetate (3 x 100 mL), washed and dried with brine and magnesium sulfate respectively. The organic extracts were collected and the solvent was removed by vacuum distillation and then under a stream of nitrogen. The products were purified using silica gel chromatography using a hexane/ethyl acetate stepwise gradient ranging from 90:10 to 60:40 hexane to ethyl acetate (EtOAc) with a 2.5% increase in the amount of EtOAc every 50 mL.

The purified products (ranging from 1~10 mg) were dissolved in $CDCl_3$ and characterised by NMR spectroscopy (Fig. S5). Minor products were identified via GC coelution or comparison of the MS spectra of standards published by others (Fig. S4).

NMR Data

Data for (2-ethylphenyl)methanol: ^{1}H NMR (500 MHz, $CDCl_3$) δ 7.35 (d, J = 6.6 Hz, 1H, H6), 7.24 (d, J = 7.6 Hz, 1H, H3) 7.18-7.12 (m, 2H, H4 & H5), 4.52 (s, 2H, 2 x H7), 2.60 (*q*, J = 7.9 Hz, 2H, 2 x H8), 1.14 (*t*, J = 7.9 Hz, 3H, 3 x H9).

Data for 1-(3-methylphenyl)ethanol: ^{1}H NMR (500 MHz, $CDCl_3$) δ 7.23 (d, J = 7.5 Hz, 1H, H6) 7.20 (s, 1H, H2), 7.18 – 7.16 (m, 1H, H5), 7.09 (d, J = 7.4 Hz, 1H, H4), 4.87 (q, J = 6.5 Hz, 1H, H7), 2.36 (s, 3H, 3 x H9), 1.5 (d, J = 6.5 Hz, 3H, 3 x H8).

Data for 2-ethyl-4-methylphenol: ^{1}H NMR (500 MHz, $CDCl_3$) δ 6.94 (s, 1H, H3), 6.89 (d, J = 8.1 Hz, 1H, H6), 6.68 (d, J = 8.1 Hz, 1H, H5), 2.54 (*q*, J = 7.6 Hz, 2H, 2 x H7), 2.22 (s, 3H, 3 x H9), 1.18 (*t*, J = 7.6 Hz, 3H, 3 x H8).

Data for 1-methyl-2-naphthalenemethanol: ^{1}H NMR (500 MHz, $CDCl_3$) δ 8.08 (d, J = 8.6 Hz, 1H, H5), 7.83 (d, J = 8.8 Hz, 1H, H4), 7.72 (d, J = 8.4 Hz, 1H, H8), 7.54 – 7.45 (m, 3H, H6, H7, H3), 4.91 (s, 2H, H12), 2.71 (s, 3H, H11). ^{13}C NMR (126 MHz, $CDCl_3$) δ 134.87 (C2), 131.15 (C4), 129.16 (C8), 129.05 (C6), 128.68 (C7), 128.19 (C3), 127.78 (C1), 126.81 (C5), 67.01 (C12), 16.55 (C11).

Data for 5-methyl-1-naphthalenemethanol: ^{1}H NMR (500 MHz, $CDCl_3$) δ 8.04 – 8.00 (m, 2H, H4 & H8), 7.56 (d, J = 6.9 Hz, 1H, H2), 7.53 – 7.43 (m, 2H, H3 & H7), 7.37 (d, J = 7.6 Hz, 1H, H6), 5.18 (s, 2H, 2 x H11), 2.73 (s, 3H, H12).

Data for 6-methyl-2-naphthalenemethanol: ^{1}H NMR (500 MHz, $CDCl_3$) δ 7.77 (s, 1H, H1), 7.76 (d, J = 3.1 Hz, 1H, H8), 7.75 – 7.73 (m, 1H, H4), 7.62 (s, 1H, H1, H5), 7.46 (dd, J = 8.3, 1.6 Hz, 1H, H7) 7.34 (dd, J = 8.3, 1.5 Hz, 1H, H3), 4.85 (s, 2H, 2 x H11), 2.53 (s, 3H, 3 x H12). ^{13}C NMR (126 MHz, CDCl3) δ 140.02 (C9), 138.25 (C10), 135.83 (C2), 134.24 (C6), 131.13 (C3), 130.37 (C8), 130.33 (C4), 129.36 (C5), 127.98 (C7), 127.92 (C1), 68.27 (C11), 24.36 (C12).

Data for 3-biphenylmethanol [15d]: ^{1}H NMR (500 MHz, $CDCl_3$) δ 7.64 – 7.57 (m, 3H), 7.53 (m, 1H), 7.64 – 7.57 (m, 3H), 7.39 – 7.31 (m, 2H), 4.77 (s, 2H).

Data for 2-(7-methylnaphthyl)methanol [15d]: ^{1}H NMR (500 MHz, d^6-acetone) δ 7.79 (s, 1H), 7.77 (m, 1H), 7.75 (m, 1H), 7.63 (s, 1H), 7.46 (m, 1H), 7.33 (m, 1H), 4.77 (s, 2H), 2.48 (s, 3H).

Data for 1-acenaphthol [29]: ^{1}H NMR (500 MHz, $CDCl_3$) δ 7.76 – 7.74 (m, 1H, H6), 7.67 (d, J = 8.2 Hz, 1H, H8), 7.58 – 7.53 (m, 2H, H5 & H10), 7.52 – 7.47 (m, 1H, H9), 7.31 (d, J = 6.8 Hz, 1H, H4), 5.75 (d, J = 7.5 Hz, 1H, H1), 3.82 (dd, J = 17.9, 7.5 Hz, 1H, H2), 3.26 (d, J = 17.8 Hz, 1H, H2). ^{13}C NMR (126 MHz, $CDCl_3$) δ 148.34 (C11), 144.19 (C3), 139.81 (C12), 133.86 (C7), 130.88 (C9), 130.69 (C5), 127.67 (C6), 125.39 (C8), 122.95 (C10), 122.51 (C4), 77.09 (C1), 44.59 (C2).

Acknowledgements

Md.R.S. thanks the University of Adelaide for an International PhD scholarship. J.H.Z.L acknowledges an Australian Government Research Training Program Scholarship (M. Phil). S.G.B. acknowledges the ARC for a Future Fellowship (FT140100355).

Keywords: biocatalysis • enzyme catalysis • protein engineering • monooxygenases • regioselectivity

[1] a) C. J. C. Whitehouse, S. G. Bell and L.-L. Wong, *Chem. Soc. Rev.* **2012**, *41*, 1218-1260; b) V. B. Urlacher and S. Eiben, *Trends Biotechnol.* **2006**, *24*, 324-330; c) J. E. Stok, K. E. Slessor, A. J. Farlow, D. B. Hawkes and J. J. De Voss in *Cytochrome P450cin (CYP176A1)*, Eds.: E. G. Hrycay and S. M. Bandiera), Springer International Publishing, Cham, **2015**, pp. 319-339; d) P. R. Ortiz de Montellano in *Substrate Oxidation by Cytochrome P450 Enzymes*, (Ed. P. R. Ortiz de Montellano), Springer International Publishing, Cham, **2015**, pp. 111-176; e) R. Bernhardt and V. B. Urlacher, *Appl. Microbiol. Biotechnol.* **2014**, *98*, 6185-6203; f) R. Bernhardt, *J. Biotechnol.* **2006**, *124*, 128-145; g) S. G. Bell, N. Hoskins, C. J. C. Whitehouse and L. L. Wong in *Design and Engineering of Cytochrome P450 Systems*, John Wiley & Sons, Ltd, **2007**, pp. 437-476; h) K. Auclair and V. Polic, *Adv. Exp. Med. Bio.* **2015**, *851*, 209-228.

[2] a) S. G. Bell and L. L. Wong, *Biochem. Biophys. Res. Commun.* **2007**, *360*, 666-672; b) D. Monti, G. Ottolina, G. Carrea and S. Riva, *Chem. Rev.* **2011**, *111*, 4111-4140; c) K. Syed, A. Porollo, Y. W. Lam, P. E. Grimmett and J. S. Yadav, *Appl. Environ. Microbiol.* **2013**, *79*, 2692-2702.

[3] F. Hannemann, A. Bichet, K. M. Ewen and R. Bernhardt, *Biochim. Biophys. Acta* **2007**, *1770*, 330-344.

[4] a) G. D. Roiban and M. T. Reetz, *Chem. Commun.* **2015**, *51*, 2208-2224; b) K. Zhang, B. M. Shafer, M. D. Demars, 2nd, H. A. Stern and R. Fasan, *J. Am. Chem. Soc.* **2012**, *134*, 18695-18704; c) S. G. Bell, F. Xu, E. O. Johnson, I. M. Forward, M. Bartlam, Z. Rao and L. L. Wong, *J. Biol. Inorg. Chem.* **2010**, *15*, 315-328; d) M. R. Sarkar, E. A. Hall, S. Dasgupta and S. G. Bell, *ChemistrySelect* **2016**, *1*, 6700-6707; e) S. G. Bell, X. Chen, R. J. Sowden, F. Xu, J. N. Williams, L. L. Wong and Z. Rao, *J. Am. Chem. Soc.* **2003**, *125*, 705-714; f) S. G. Bell, W. Yang, J. A. Yorke, W. Zhou, H. Wang, J. Harmer, R. Copley, A. Zhang, R. Zhou, M. Bartlam, Z. Rao and L. L. Wong, *Acta Crystallogr. D Biol. Crystallogr.* **2012**, *68*, 277-291.

[5] a) M. J. Pecyna, R. Ullrich, B. Bittner, A. Clemens, K. Scheibner, R. Schubert and M. Hofrichter, *Appl. Microbiol. Biotechnol.* **2009**, *84*, 885-897; b) A. Dennig, N. Lulsdorf, H. Liu and U. Schwaneberg, *Angew. Chem. Int. Ed. Engl.* **2013**, *52*, 8459-8462; c) S. Kille, F. E. Zilly, J. P. Acevedo and M. T. Reetz, *Nat Chem* **2011**, *3*, 738-743.

[6] a) C. F. Harford-Cross, A. B. Carmichael, F. K. Allan, P. A. England, D. A. Rouch and L. L. Wong, *Protein Eng.* **2000**, *13*, 121-128; b) S. G. Bell, C. F. Harford-Cross and L. L. Wong, *Protein Eng.* **2001**, *14*, 797-802; c) P. A. England, C. F. Harford-Cross, J. A. Stevenson, D. A. Rouch and L. L. Wong, *FEBS Lett.* **1998**, *424*, 271-274; d) T. L. Poulos, B. C. Finzel and A. J. Howard,

J. Mol. Biol. **1987**, *195*, 687-700; e) M. Katagiri, B. N. Ganguli and I. C. Gunsalus, *J. Biol. Chem.* **1968**, *243*, 3543-3546.
[7] a) C. Y. Lin, A. M. Wheelock, D. Morin, R. M. Baldwin, M. G. Lee, A. Taff, C. Plopper, A. Buckpitt and A. Rohde, *Toxicology* **2009**, *260*, 16-27; b) A. Belles, C. Alary, J. Criquet and G. Billon, *Chemosphere* **2016**, *164*, 347-354.
[8] a) K. Hunger and W. Herbst in *Pigments, Organic*, Wiley-VCH Verlag GmbH & Co. KGaA, **2000**; b) K. Griesbaum, A. Behr, D. Biedenkapp, H.-W. Voges, D. Garbe, C. Paetz, G. Collin, D. Mayer and H. Höke in *Hydrocarbons*, Wiley-VCH Verlag GmbH & Co. KGaA, **2000**; c) M. Greene in *Perylene Pigments*, Wiley-VCH Verlag GmbH & Co. KGaA, **2009**, pp. 261-274.
[9] A. B. Carmichael and L. L. Wong, *Eur. J. Biochem.* **2001**, *268*, 3117-3125.
[10] T. Makino, T. Otomatsu, K. Shindo, E. Kitamura, G. Sandmann, H. Harada and N. Misawa, *Microb. Cell. Fact.* **2012**, *11*, 95.
[11] a) N. Misawa, M. Nodate, T. Otomatsu, K. Shimizu, C. Kaido, M. Kikuta, A. Ideno, H. Ikenaga, J. Ogawa, S. Shimizu and K. Shindo, *Appl. Microbiol. Biotechnol.* **2011**, *90*, 147-157; b) M. J. Schocken and D. T. Gibson, *Appl. Environ. Microbiol.* **1984**, *48*, 10-16.
[12] a) S. M. Fowler, P. A. England, A. C. G. Westlake, D. R. Rouch, D. P. Nickerson, C. Blunt, D. Braybrook, S. West, L.-L. Wong and S. L. Flitsch, *Chem. Commun.* **1994**, 2761-2762; b) C. J. Whitehouse, S. G. Bell and L. L. Wong, *Chem. Eur. J.* **2008**, *14*, 10905-10908; c) C. J. Whitehouse, N. H. Rees, S. G. Bell and L. L. Wong, *Chem. Eur. J.* **2011**, *17*, 6862-6868; d) Q. S. Li, J. Ogawa, R. D. Schmid and S. Shimizu, *Appl. Environ. Microbiol.* **2001**, *67*, 5735-5739; e) O. Sibbesen, Z. Zhang and P. R. Ortiz de Montellano, *Arch. Biochem. Biophys.* **1998**, *353*, 285-296.
[13] a) J. K. Fredrickson, D. L. Balkwill, G. R. Drake, M. F. Romine, D. B. Ringelberg and D. C. White, *Appl. Environ. Microbiol.* **1995**, *61*, 1917-1922; b) Y. Lyu, W. Zheng, T. Zheng and Y. Tian, *PLoS One* **2014**, *9*, e101438.
[14] a) S. G. Bell, A. Dale, N. H. Rees and L. L. Wong, *Appl. Microbiol. Biotechnol.* **2010**, *86*, 163-175; b) W. Yang, S. G. Bell, H. Wang, W. Zhou, N. Hoskins, A. Dale, M. Bartlam, L. L. Wong and Z. Rao, *J. Biol. Chem.* **2010**, *285*, 27372-27384.
[15] a) E. A. Hall, M. R. Sarkar, J. H. Z. Lee, S. D. Munday and S. G. Bell, *ACS Catal.* **2016**, *6*, 6306-6317; b) S. G. Bell, W. Yang, A. Dale, W. Zhou and L.-L. Wong, *Appl. Microbiol. Biotechnol.* **2013**, *97*, 3979-3990; c) E. A. Hall and S. G. Bell, *RSC Adv.* **2015**, *5*, 5762-5773; d) E. A. Hall, M. R. Sarkar and S. G. Bell, *Cat. Sci. Technol.* **2017**, **7**, 1537-1548.
[16] a) R. Fasan, *ACS Catal.* **2012**, *2*, 647-666; b) J. A. McIntosh, C. C. Farwell and F. H. Arnold, *Curr. Opin. Chem. Biol.* **2014**, *19*, 126-134; c) E. O'Reilly, V. Kohler, S. L. Flitsch and N. J. Turner, *Chem. Commun.* **2011**, *47*, 2490-2501.
[17] a) M. Ma, S. G. Bell, W. Yang, Y. Hao, N. H. Rees, M. Bartlam, W. Zhou, L. L. Wong and Z. Rao, *Chembiochem* **2011**, *12*, 88-99; b) W. Yang, S. G. Bell, H. Wang, W. Zhou, M. Bartlam, L. L. Wong and Z. Rao, *Biochem. J.* **2011**, *433*, 85-93; c) S. Vohra, M. Musgaard, S. G. Bell, L. L. Wong, W. Zhou and P. C. Biggin, *Protein Sci.* **2013**, *22*, 1218-1229.
[18] a) S. G. Bell, D. A. Rouch and L.-L. Wong, *J. Mol. Catal. B: Enzym.* **1997**, *3*, 293-302; b) S. K. Manna and S. Mazumdar, *Dalton Trans.* **2010**, *39*, 3115-3123; c) P. J. Loida and S. G. Sligar, *Biochemistry* **1993**, *32*, 11530-11538; d) P. P. Kelly, A. Eichler, S. Herter, D. C. Kranz, N. J. Turner and S. L. Flitsch, *Beilstein J. Org. Chem.* **2015**, *11*, 1713-1720.
[19] S. D. Munday, S. Dezvarei, I. C. K. Lau and S. G. Bell, *ChemCatChem* **2017**, *9*, 2512-2522.
[20] E. J. Corey and M. Sodeoka, *Tetrahedron Lett.* **1991**, *32*, 7005-7008.
[21] S. D. Munday, S. Dezvarei and S. G. Bell, *ChemCatChem* **2016**, *8*, 2789-2796.
[22] a) H. Greenland, J. Pinhey and S. Sternhell, *Aus. J. Chem.* **1987**, *40*, 325-331; b) D. García, F. Foubelo and M. Yus, *Tetrahedron* **2008**, *64*, 4275-4286.
[23] a) S. G. Sligar, *Biochemistry* **1976**, *15*, 5399-5406; b) S. G. Sligar and I. C. Gunsalus, *Proc. Natl. Acad. Sci. U. S. A.* **1976**, *73*, 1078-1082; c) M. J. Honeychurch, H. A. O. Hill and L. L. Wong, *FEBS Lett.* **1999**, *451*, 351-353.
[24] A. M. Colthart, D. R. Tietz, Y. Ni, J. L. Friedman, M. Dang and T. C. Pochapsky, *Sci. Rep.* **2016**, *6*, 22035.
[25] J. Sambrook, E. F. Fritsch and T. Maniatis, *Molecular Cloning: A Laboratory Manual*, Cold Spring Harbor Laboratory Press, New York, **1989**, p.
[26] a) K. Arnold, L. Bordoli, J. Kopp and T. Schwede, *Bioinformatics* **2006**, *22*, 195-201; b) M. Biasini, S. Bienert, A. Waterhouse, K. Arnold, G. Studer, T. Schmidt, F. Kiefer, T. Gallo Cassarino, M. Bertoni, L. Bordoli and T. Schwede, *Nucleic Acids Res.* **2014**, *42*, W252-258.
[27] a) N. K. Maddigan and S. G. Bell, *Arch. Biochem. Biophys.* **2017**, *615*, 15-21; b) I. C. Gunsalus, J. R. Meeks and J. D. Lipscomb, *Ann. N. Y. Acad. Sci.* **1973**, *212*, 107-121.
[28] J. W. Williams and J. F. Morrison, *Methods Enzymol.* **1979**, *63*, 437-467.
[29] J. V. Pothuluri, J. P. Freeman, F. E. Evans and C. E. Cerniglia, *Appl. Environ. Microbiol.* **1992**, *58*, 3654-3659.

10.1002/cbic.201700316

WILEY-VCH

Entry for the Table of Contents

FULL PAPER

The CYP101B1 enzyme from the bacteria *Novosphingobium aromaticivorans* has been engineered to better bind and oxidise hydrophobic aromatic substrates. Histidine 85 was identified as a potential active site residue by sequence alignment. The H85F variant improved activity and offered unusual selectivity options.

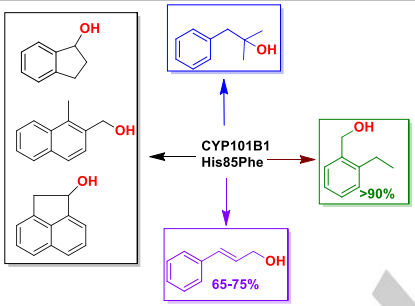

*Md. Raihan Sarkar, Joel H.-Z. Lee and Dr. Stephen G. Bell**

Page No. – Page No.

The oxidation of hydrophobic aromatic substrates using a variant of the P450 monooxygenase CYP101B1